DEVELOPMENT OF NMR IMAGING PROBES FOR ADVANCED CERAMICS

N. Gopalsami, G.A. Forster, S.L. Dieckman, and W.A. Ellingson
Materials and Components Technology Division

R.E. Botto

Chemistry Division
Argonne National Laboratory
Argonne, Illinois 60439

INTRODUCTION

Nuclear magnetic resonance imaging (NMRI) holds the potential for the non-destructive evaluation of ceramics and for the improvement of ceramic processing in general. It can provide valuable diagnostic information about the spatial variations of binders, plasticizers, sintering aids, deflocculants, and other organics in injection-molded and slip-cast green ceramics. Poor distribution of these organics, after subsequent processing steps such as sintering, hot isostatic pressing, and machining, can lead to final parts that are defective and/or with poor mechanical properties.

Despite the advances in NMRI in the medical area, few efforts [1-4] have been made to apply NMRI to materials studies because of the need for special imaging probes and techniques. A major difference between the two applications is in the line widths of NMR spectra. For example, the line width of proton spectra from the organics in green ceramic materials [2] is about 2500 Hz, compared to a few Hz in biological systems. Because linear gradient fields are used in NMR imaging to frequency-label spatial positions, the gradient strength required to resolve two positions in space must be high enough to ensure that the difference in the resonance frequencies between these two positions is greater than the line widths of the resonances. The imaging of ceramics with a spatial resolution of 100 μm, for example, would require a gradient strength of 50 G/cm.

Another difference is in the imaging technique. While spin-warp imaging is used in medical systems, the method of choice for materials with short spin-spin relaxation time, T_2, (large line widths correspond to short T_2) is back-projection. This method allows the NMR response (FID) to be detected immediately after the RF excitation, thus preserving the maximum signal intensity. Back-projection, however, poses more stringent specifications on the probe design, requiring (1) highly uniform gradient and RF fields, (2) well-balanced gradient fields between the orthogonal axes, and (3) strict alignment of the static, gradient, and RF fields with respect to the center of the sample space. Also, the RF bandwidth must be great enough to span the entire range of frequencies produced by the gradient fields. This paper presents the design and test results of a special imaging probe built at Argonne to meet these requirements for ceramics characterization.

PROBE DESIGN

The imaging probe (Fig. 1) is designed to be used in an 89-mm vertical bore, 2.35-T superconducting magnet in conjunction with a Bruker CXP-100

Review of Progress in Quantitative Nondestructive Evaluation, Vol. 9
Edited by D.O. Thompson and D.E. Chimenti
Plenum Press, New York, 1990

spectrometer. The probe must accommodate samples up to 28 mm in diameter to meet our present requirements. The probe includes an RF coil for excitation and detection of the nuclear signals, and a set of coils to create orthogonal gradient fields with respect to the x, y, and z spatial coordinates. To improve the filling factor of the RF coil, the probe allows emplacement of different-sized RF coils (<30 mm), depending on the sample size. At high field strengths, the gradient coils will generate considerable heat because of resistive losses; hence, provision is made for cooling the probe.

Gradient Coils

The coil design uses a saddle-type configuration for the x and y gradients and a pair of Maxwell coils for the z gradient [5], as shown in Fig. 2. The design of the coils was based on a finite-element analysis of the fields with the computer code OPERA/TOSCA from Vector Fields. Appropriate grooves were machined on an epoxy-glass tube to accommodate the windings, and the coils were wound in two layers with 12 turns each of AWG 22 copper wire. They were then tested by driving with constant currents from a Techron power amplifier and measuring the magnetic fields along the x, y, and z axes with a Hall probe. The simulated results are shown in Fig. 3. For all three gradients, the simulated fields show good agreement with the measured fields. The projected gradient strength of the fields is 48 G/cm at the maximum coil rating of 20 A at a 10% duty cycle.

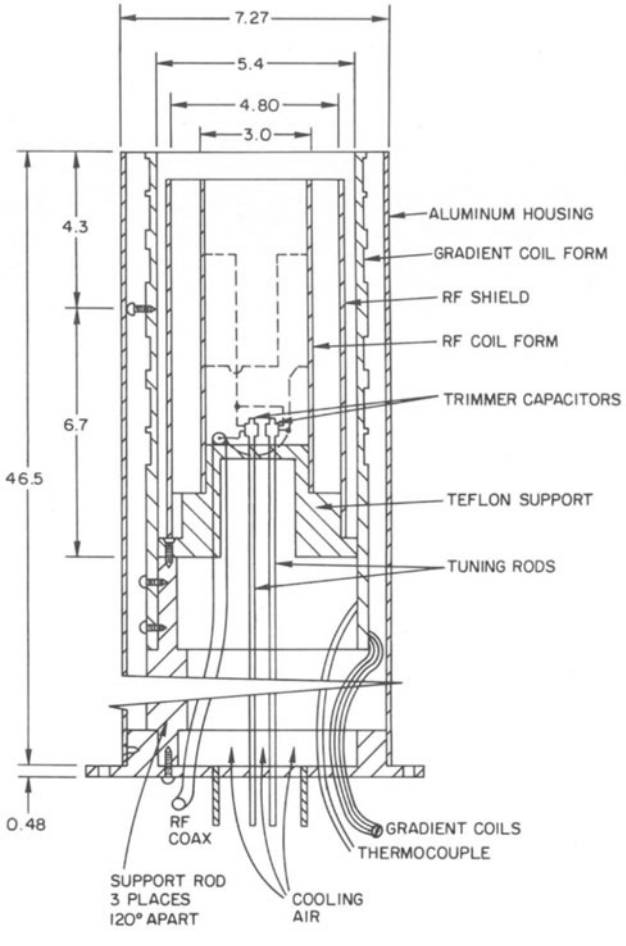

Fig. 1. Probe Assembly (Dimensions in cm)

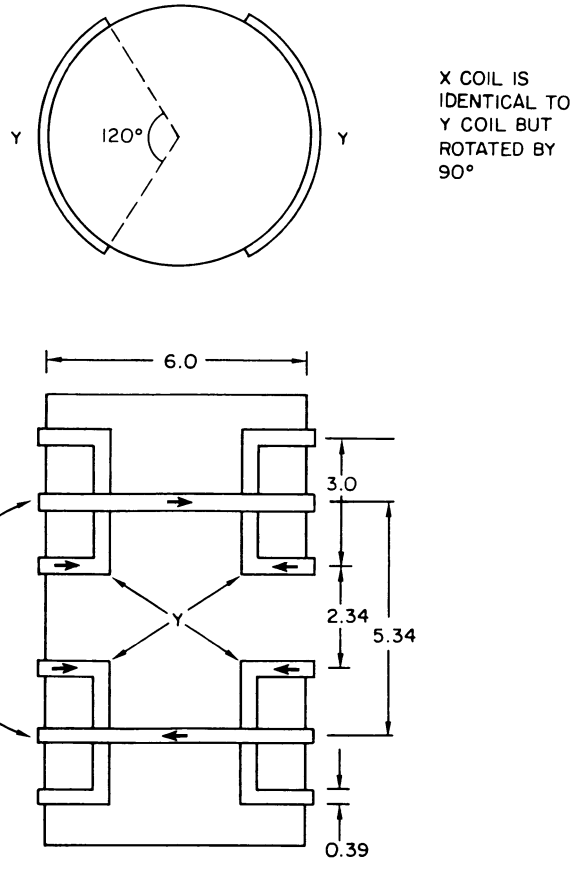

Fig. 2. Gradient Coil Geometry (Dimensions in cm)

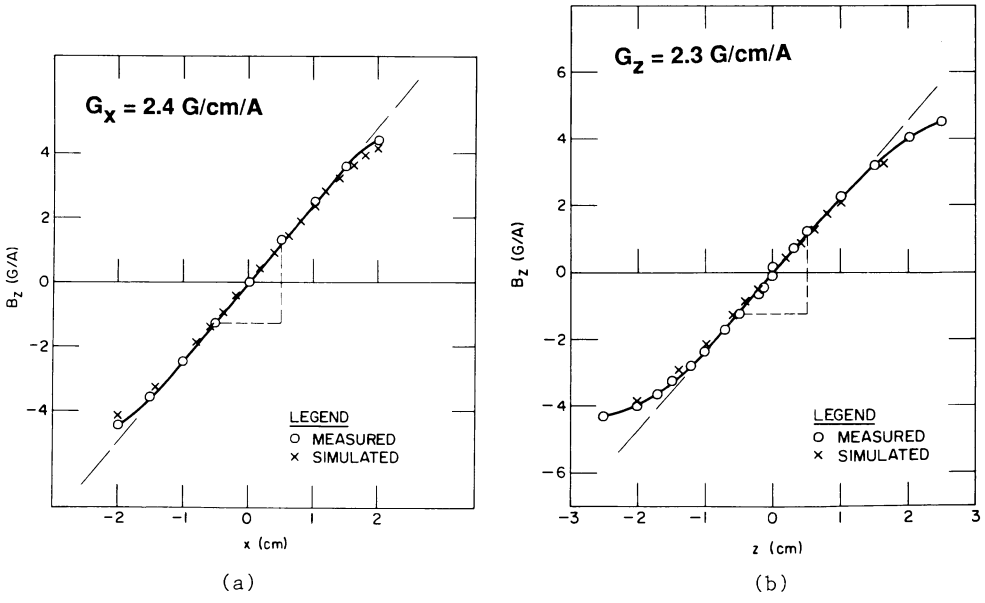

Fig. 3. (a) X (or Y) Gradient Field; (b) Z Gradient Field

RF Coil

An RF coil must efficiently transmit RF power to the sample volume to excite the nuclear spins and to detect the precessing nuclear magnetization with a high signal-to-noise ratio. The main design requirements of the RF coil are that it should resonate at the desired operating frequency with a high Q, produce a homogeneous magnetic field transverse to the main magnetic axis, and provide a good filling factor. The saddle-type RF coil design [6] shown in Fig. 4 satisfies these requirements in the frequency range of interest (100 MHz) and also allows convenient loading of the samples. A single-turn coil was wound on a 30-mm outside diameter NMR glass tube, and its resonant characteristics were tested. A tuning and matching circuit (Fig. 5a) was constructed so the coil can be resonated at the operating frequency of about 100 MHz and its impedance matched to 50 Ω, which is the characteristic impedance of the coaxial cable that connects the coil to the transmitter and receiver circuits of the spectrometer. Figure 5b shows the resonant behavior of the circuit; a quality factor (Q) of 239 was obtained with no sample inside the coil.

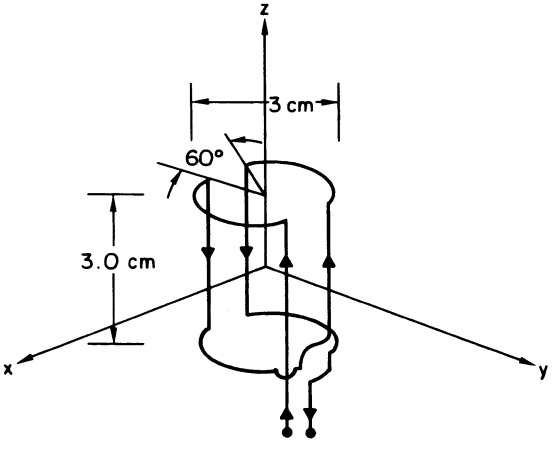

Fig. 4. RF Coil Geometry

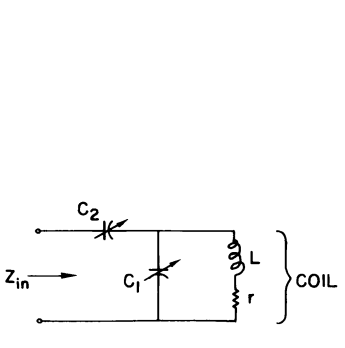

(a)

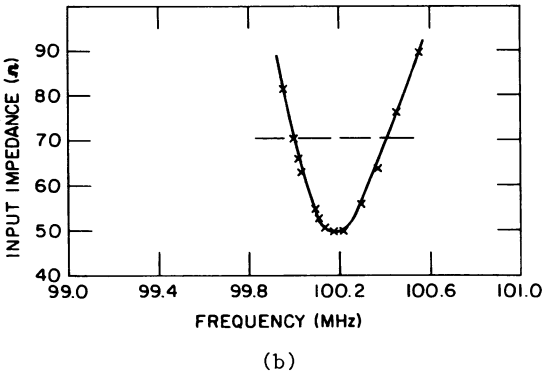

(b)

Fig. 5. Measurement of RF Coil Resonance (No sample): (a) Tuning and matching circuit; (b) RF coil resonance

TEST RESULTS

Figure 6 is a block diagram of the Argonne NMRI system. An IBM-PC-based pulse programmer (also home-built), using trigger pulses from the spectrometer, provides gradient control pulses. The pulse programmer has the flexibility to generate a variety of pulse protocols along with RF pulse shaping. Three Techron power amplifiers (DC-45 kHz; 2kVA) drive the gradient coils in the constant-current mode based on the gradient pulses from the pulse programmer. NMR data are acquired on the Bruker spectrometer and then transported from its Aspect 3000 computer to a VAX 8700 computer via Ethernet for image reconstruction and processing. Image reconstruction is done by a back-projection imaging software developed at Argonne and based on the Donner algorithms for reconstruction tomography [7].

NMR Imaging of Green Ceramics

The efficacy of the probe for ceramics characterization is tested by imaging modulus-of-rupture (MOR) test bars (made of injection-molded Si_3N_4; see Fig. 7 for size) supplied by the Garrett Ceramic Components Division. A two-turn 20-mm RF coil instead of the 30-mm coil described earlier, was used to improve the filling factor and hence the signal-to-noise ratio. A resolution phantom was prepared by drilling holes of various sizes in a test bar (Fig. 7). Back-projection images of protons from the organics in the bar were produced in the x-z plane (no slice selection along the thickness of the bar). A total of 90 projections and 128 averages were used for each image. Figure 8 shows two NMR images of the resolution phantom corresponding to gradient strengths of 3.6 and 7.2 G/cm. Adjacent to the resolution phantom is the image of an intensity standard (a small section of an MOR bar placed next to the test bar). Clearly, the holes in the phantom are well-resolved at 7.2 G/cm except for the smallest hole (1.02 mm) at the bottom, which is barely visible. The two upper holes are not in the field of view. Based on this test, projected resolution with 50-G/cm gradient strength is 175 μm.

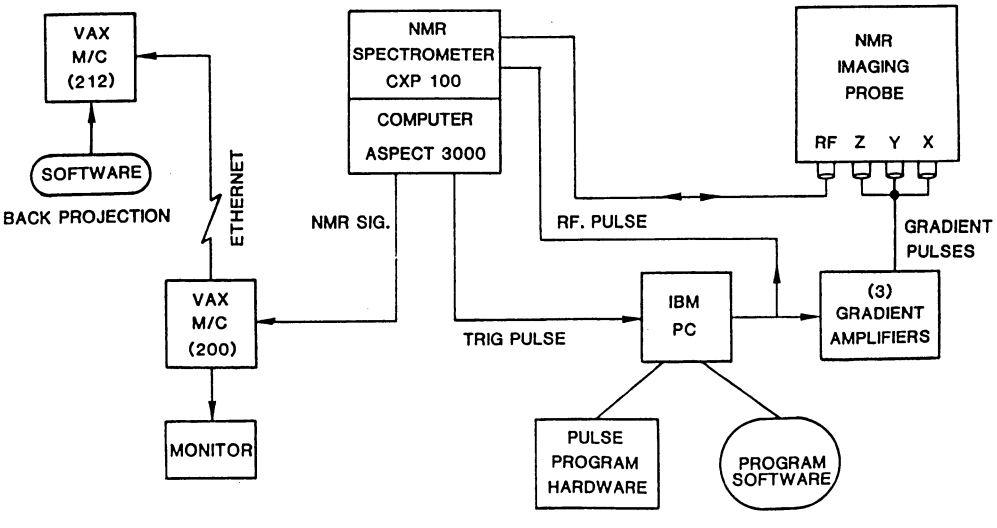

Fig. 6. Block Diagram of NMR Imaging System

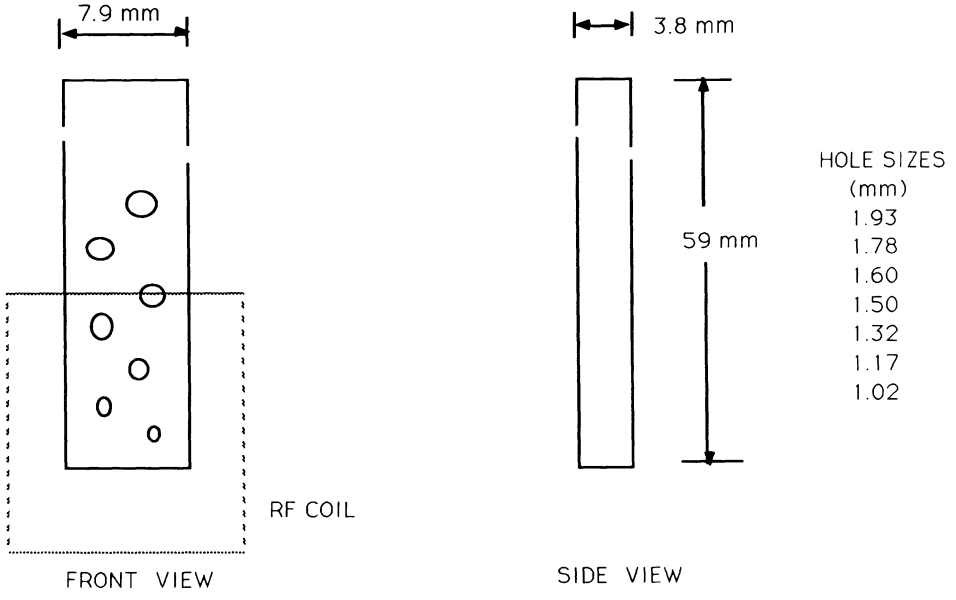

Fig. 7. Resolution Phantom

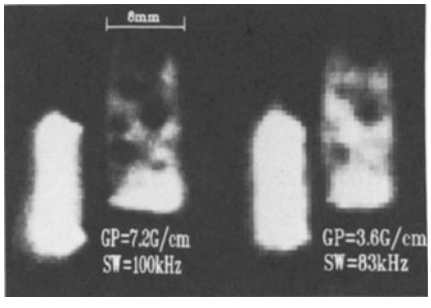

Fig. 8. Effect of Gradient Strength on Resolution

To determine the NMR sensitivity to changes in organics concentration, we fabricated two concentration phantoms by cold-processing Si_3N_4 mixtures with known weight percent of organics in the form of small disks (4.8 mm diameter and 3 mm thick). The disks were weighed and inserted in a Teflon holder that was identical in geometry to the MOR bars. Figure 9 shows back-projection images of the concentration phantoms, with three cold-pressed disks per phantom. Each phantom was placed vertically along the z axis of the RF coil, and the vertical location of some of the disks extended beyond the good field region (~0.7 times the radius) of the coil. Consequently, we must take into account the fact that image intensity would roll off above the good field region. The roll-off curve was determined by imaging an MOR bar with a uniform concentration of organics. After correcting for the roll-off behavior and normalizing the image intensities of the two phatoms using the intensity standard, we plotted the grey-scale intensities of the disks as shown in Fig. 10. It is clear that the image intensity increases with weight-percent of organics. The large spread of the data about the linear fit is attributed to inaccuracies in the preparation and calibration of the phantoms.

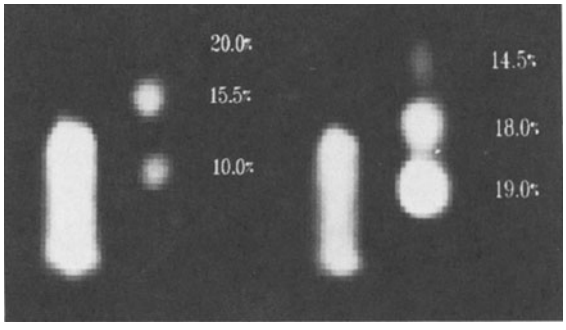

Fig. 9. Nonnormalized Images of Different wt.% of Organics in Cold Pressed Si_3N_4 Pellets

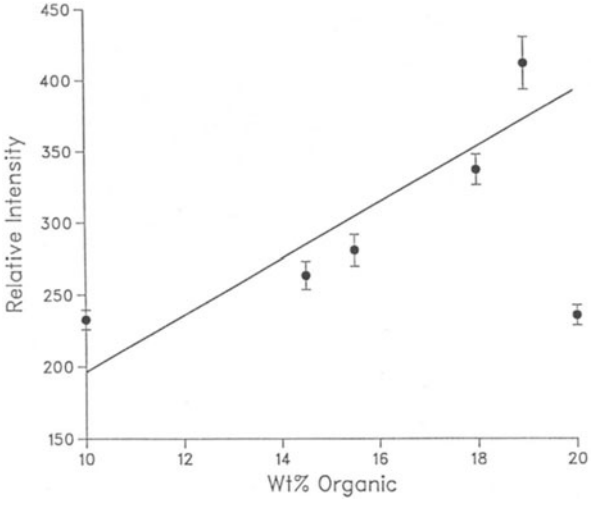

Fig. 10. Image Intensity vs. wt.% Organic in Green Silicon Nitride Standards

CONCLUSIONS

An NMR imaging probe was designed and tested for the characterization of advanced ceramics. Accommodating samples up to 28 mm, the probe can generate gradient fields of strength up to 50 G/cm and provide a spatial resolution of 0.175 mm in green ceramics. Successful NMR images of injection-molded Si_3N_4 green bars have been produced using filtered back-projection. Preliminary results indicate that changes in the organics concentration of Si_3N_4 bars can be detected with a sensitivity of 1 wt.% from the grey-scale intensities of the NMR images.

ACKNOWLEDGMENTS

The authors wish to thank R.J. Lari from Vector Fields Inc. for magnetic field calculations, and M. Szuster for fabrication of concentration phantoms. This work was supported by the U.S. Department of Energy, Office of Fossil Energy, AR&TD Materials Program; and Assistant Secretary for Conservation and Renewal Energy, Office of Transportation

Systems; as part of the Ceramics Technology for Advanced Heat Engines Project of the Advanced Materials Development Program, under Contract W-31-109-Eng-38.

REFERENCES

1. J. M. Listerud, S. W. Sinton, and G. P. Drobny, Analy. Chem., 61, 23 (1989).

2. W. A. Ellingson, J. L. Ackerman, L. Garrido, P. S. Wong, and S. Gronmeyer, Argonne National Laboratory Report ANL-87-53 (1988).

3. G. C. Chingas, S. B. Miller, and A. N. Garroway, J. Magn. Reson. 66, 530 (1986).

4. D. G. Cory, J. W. M. van Os, and W. S. Veeman, J. Magn. Reson., 76, 543 (1988).

5. S. R. Thomas, L. J. Busse, and J. F. Schenek, in NMR in Medicine, edited by S. R. Thomas and R. L. Dixon (American Institute of Physics 1986).

6. D. L. Hoult, Progr. in NMR Spectr., 12, 41 (1978).

7. R. H. Huesman, G. T. Gullburg, W. L. Greenberg, and T. S. Budinger, Lawrence Berkeley Laboratory Report PUB-214 (1977).